Am J Physiol Lung Cell Mol Physiol 288: L398–L408, 2005.
First published October 29, 2004; doi:10.1152/ajplung.00299.2004.

Voltage-gated proton channels help regulate pH_i in rat alveolar epithelium

Ricardo Murphy, Vladimir V. Cherny, Deri Morgan, and Thomas E. DeCoursey

Department of Molecular Biophysics and Physiology, Rush University Medical Center, Chicago, Illinois

Submitted 9 August 2004; accepted in final form 25 October 2004

Murphy, Ricardo, Vladimir V. Cherny, Deri Morgan, and Thomas E. DeCoursey. Voltage-gated proton channels help regulate pH_i in rat alveolar epithelium. *Am J Physiol Lung Cell Mol Physiol* 288: L398–L408, 2005. First published October 29, 2004; doi: 10.1152/ajplung.00299.2004.—Voltage-gated proton channels are expressed highly in rat alveolar epithelial cells. Here we investigated whether these channels contribute to pH regulation. The intracellular pH (pH_i) was monitored using BCECF in cultured alveolar epithelial cell monolayers and found to be 7.13 in nominally HCO_3^--free solutions [at external pH (pH_o) 7.4]. Cells were acid-loaded by the NH_4^+ prepulse technique, and the recovery was observed. Under conditions designed to eliminate the contribution of other transporters that alter pH, addition of 10 μM $ZnCl_2$, a proton channel inhibitor, slowed recovery about twofold. In addition, the pH_i minimum was lower, and the time to nadir was increased. Slowing of recovery by $ZnCl_2$ was observed at pH_o 7.4 and pH_o 8.0 and in normal and high-K^+ Ringer solutions. The observed rate of Zn^{2+}-sensitive pH_i recovery required activation of a small fraction of the available proton conductance. We conclude that proton channels contribute to pH_i recovery after an acid load in rat alveolar epithelial cells. Addition of $ZnCl_2$ had no effect on pH_i in unchallenged cells, consistent with the expectation that proton channels are not open in resting cells. After inhibition of all known pH regulators, slow pH_i recovery persisted, suggesting the existence of a yet-undefined acid extrusion mechanism in these cells.

proton conductance; pH regulation; hydrogen ion; acid load; 2′,7′-bis(2-carboxyethyl)-5(6)-carboxyfluorescein; intracellular pH

ALVEOLAR TYPE II EPITHELIAL CELLS exhibit an impressive panoply of pH-regulating mechanisms, perhaps reflecting their role in extruding enormous quantities of acid in the form of CO_2 during respiration as well as their exposure to an asymmetrical pH environment. Whereas the basolateral membranes face typical interstitial fluid, the apical membranes face the alveolar subphase, the fluid at the interface between air and tissues in the alveolus. This fluid is highly acidic compared with plasma or interstitial fluid, with estimates at pH 6.69 in dog lung (17), pH 6.27 in fetal lamb lung (1), and pH 6.92 in rabbit lung (31). The properties and localization of several transporters that influence pH_i have been studied previously. Sodium-proton exchange, Na^+/H^+-antiport, is active at pH_i <7.0 during recovery from an acid load (32) and appears to be localized in basolateral membranes (22, 26). Sodium-independent Cl^-/HCO_3^- exchange contributes to recovery from an alkaline load (33), and the alveolar type II epithelial isoform is restricted to the basolateral surface of alveolar epithelial monolayers (27). A Cl^--independent Na^+-HCO_3^- symporter contributes to cytosolic alkalinization and, in contrast to Na^+/H^+-antiport, is constitutively active at intracellular pH (pH_i) >7.0 (25). The Na^+-HCO_3^- symporter is detected in basolateral membranes (27). Evidence for a K^+-H^+-ATPase exists in guinea pig but not rat type II pneumocytes (24). A plasma membrane V-type H^+-ATPase reportedly is active at physiological pH and may keep pH_i near 7.5 (28), although Brown et al. (6) found no evidence for a V-type H^+-ATPase in rat type II cells and concluded that ATP modulates Na^+/H^+-antiport. The possibility that Cl^-/OH^- exchange (38) might occur in rat alveolar epithelial cells was suggested by highly indirect evidence (13). Finally, voltage-gated proton channels comprise a major conductance in rat alveolar epithelial type II cells (10), are demonstrably present in the apical membranes of cultured cells (12), and might be present in all membranes. Proton channels are opened by membrane depolarization, decreased pH_i, increased extracellular pH (pH_o), or a combination of these factors (9, 11). Their regulation by pH and voltage ensures that these channels open only when there is an outward electrochemical gradient for protons (11). Because this gradient is normally inward (10), we predict that H^+ current inhibition with Zn^{2+} should have no effect on pH_i in unchallenged alveolar epithelial cells. In several other cells, proton channels mediate pH_i recovery after an acid load. However, until now, no direct evidence for this or any other specific function for proton channels had been demonstrated in alveolar epithelial cells. Effects of Zn^{2+} reported here indicate that voltage-gated proton channels are closed at normal pH_i but contribute to H^+ extrusion after acid loading rat alveolar epithelial type II cells.

MATERIALS AND METHODS

Rat alveolar epithelial cells. Type II alveolar epithelial cells were isolated from adult male Sprague-Dawley rats by enzyme digestion, lectin agglutination, and differential adherence, as described in detail elsewhere (15), with three exceptions. First, the solution used to perfuse the lungs is 40 ml of HBSS (catalog no. 14170-112; GIBCO Laboratories, Grand Island, NY). Second, we use 0.2 mg/ml elastase without trypsin to dissociate the cells. Third, the filtrate is centrifuged at 2,000 rpm (instead of 1,500 rpm). Before invasive procedures were initiated, the rats were anesthetized deeply with pentobarbital sodium. The rats were treated humanely in compliance with local law, our Institutional Animal Care and Use Committee, and with the National Institutes of Health Guide for the Care and Use of Laboratory Animals. The lungs were lavaged to remove macrophages, elastase was instilled, and then the tissue was minced and forced through fine gauze. Lectin agglutination and differential adherence further removed contaminating cell types. The preparation at first includes mainly type II alveolar epithelial cells, but after several days in culture, the properties of the cells are more like type I cells. Studies were done on monolayers of cells grown on cover glass chips for 5–25 days. Plotting the parameters defined in Fig. 2 against time in culture did not reveal any trends (data not shown).

Address for reprint requests and other correspondence: T. E. DeCoursey, Dept. of Molecular Biophysics and Physiology, Rush Univ. Medical Center, 1750 W. Harrison, Chicago, IL 60612 (E-mail: tdecours@rush.edu).

The costs of publication of this article were defrayed in part by the payment of page charges. The article must therefore be hereby marked "*advertisement*" in accordance with 18 U.S.C. Section 1734 solely to indicate this fact.

Chemicals. SCH-28080 and some of the 2′,7′-bis(2-carboxyethyl)-5(6)-carboxyfluorescein-acetoxymethyl ester (BCECF-AM) used here were purchased from Calbiochem (La Jolla, CA). All of the remaining chemicals, including nigericin, 5-(*N,N*-dimethyl)amiloride hydrochloride (DMA), bafilomycin A_1, and some BCECF-AM, were obtained from Sigma Chemical (St. Louis, MO).

Measurement of pH_i. Cells were loaded for 20–60 min with 10–20 μg/ml BCECF-AM, the nonfluorescent, membrane-permeant acetoxymethyl ester of BCECF dissolved in 1 ml of Ringer solution (in mM: 160 NaCl, 4.5 KCl, 2 $CaCl_2$, 1 $MgCl_2$, 5 HEPES; pH 7.4) or culture medium. Intracellular esterases cleave the three AM ester groups to form the charged, membrane-impermeant, pH-sensitive, fluorescent dye BCECF (30). pH_i was monitored ratiometrically with a model LS50B luminescence spectrometer (Perkin-Elmer, Norwalk, CT) at excitation wavelengths of 440 and 495 nm and an emission wavelength of 525 nm. Excitation and emission slit widths were 5 and 3 nm, respectively. We took background readings before loading the dye and subtracted them from the fluorescence intensities (F_λ, where λ is the excitation wavelength) before calculating the fluorescence ratio ($R = F_{495}/F_{440}$ measured at 525 nm). Because of a progressive detachment of cells from the cover glass (especially during solution changes), fluorescence intensities frequently declined over the course of an experiment. Data for which F_{440} was less than twice background were discarded.

At the end of some experiments we performed a calibration (Fig. 1*A*) using the nigericin technique (30, 39). Specifically, the tissue was transferred to solutions containing 80–100 mM KCl, 3–10 μM nigericin, 2 mM $CaCl_2$, and 100 mM buffer (pH 5.5 and 6.0, MES; 6.5, bis-Tris; 7.0, *N,N*-bis[2-hydroxyethyl]-2-aminoethanesulfonic acid; 7.55, HEPES; 8.0, Tricine). Any glassware or other apparatus that came into contact with nigericin was soaked overnight in ethanol (3). Failure to observe this precaution resulted in rapid recovery from an acid load [time constant (τ) ≈ 4 min]. In later experiments the use of disposable cuvettes obviated the need to wash cuvettes, but tissue holders were still soaked overnight in ethanol, even when nigericin was not used (as a precaution against contamination). Calibration was not possible in all experiments because of cell detachment and the consequent fall in F_λ. Accordingly, a mean calibration curve was used to calculate pH_i from the fluorescence-ratio data. We obtained this curve by fitting the following equation to data pooled from six experiments (Fig. 1*B*)

$$R = \frac{R_{max} + R_{min}10^{pK_a^* - pH}}{1 + 10^{pK_a^* - pH}} \quad (1)$$

where R_{max} is the value of R as $[H^+] \rightarrow 0$, R_{min} is the value of R as $[H^+] \rightarrow \infty$ and pK_a^* is related to the negative log of acidic dissociation constant (pK_a) of BCECF by

$$pK_a^* = pK_a + \log_{10}[F_{440}^{\infty}/F_{440}^{0}] \quad (2)$$

where F_{440}^{∞} and F_{440}^{0} are the values of F_{440} as $[H^+] \rightarrow \infty$ and $[H^+] \rightarrow 0$, respectively. Because 440 nm is close to the isosbestic point of BCECF, the log term in *Eq. 2* should be close to zero so that $pK_a^* \approx pK_a$ (provided external $[K^+]$ is chosen correctly, see Refs. 4, 5). *Equations 1* and *2* follow from the treatment of fluorescent calcium probes by Grynkiewicz et al. (21). The estimated parameter values were $pK_a^* = 7.337 \pm 0.071$, $R_{min} = 1.329 \pm 0.066$, and $R_{max} = 8.83 \pm 0.52$.

Experimental protocol. After dye loading, cells were initially placed in 1 ml of Ringer solution and were then acid-loaded by the NH_4Cl prepulse technique (35). Specifically, 250 μl of 150 mM NH_4Cl solution in water was added to the 1 ml of Ringer to give a final NH_4Cl concentration close to 30 mM. As shown in Fig. 2, this resulted in an abrupt rise in pH_i, followed by a slower decline (*phases A* and *B*). The sharp rise in pH_i is believed to reflect the rapid influx

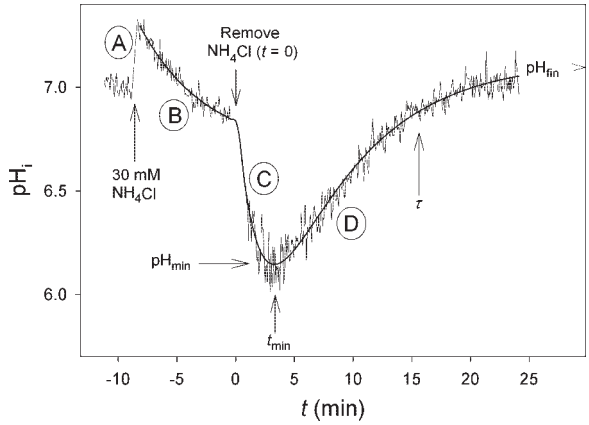

Fig. 2. An example of an acid-load/recovery cycle. The tissue was initially in Ringer. Addition of 30 mM NH_4Cl results in a transient increase in pH_i (A) associated with a rapid influx of NH_3, followed by a slower fall in pH_i as NH_4^+ enters the cells (B). On transferring the tissue to NH_4Cl-free potassium Ringer (K-Ringer) solution at time (t) = 0, pH_i falls rapidly (acid load) as NH_3 leaves the cells (C). This is followed by a slower recovery, presumably due to proton (or proton equivalent) efflux (D). The bold curve for $t > 0$ is a fit of *Eq. 3*. For $t < 0$ the data were fitted with an exponential decay. This component was not used for analysis, except to establish $pH_i(0)$ (*Eq. 3*). pH_{fin}, limiting value to which the pH apparently recovers as $t \rightarrow \infty$; t_{min}, the time to reach the pH minimum at the end of *phase C*; pH_{min}, pH at that minimum; τ, time constant of pH_i recovery.

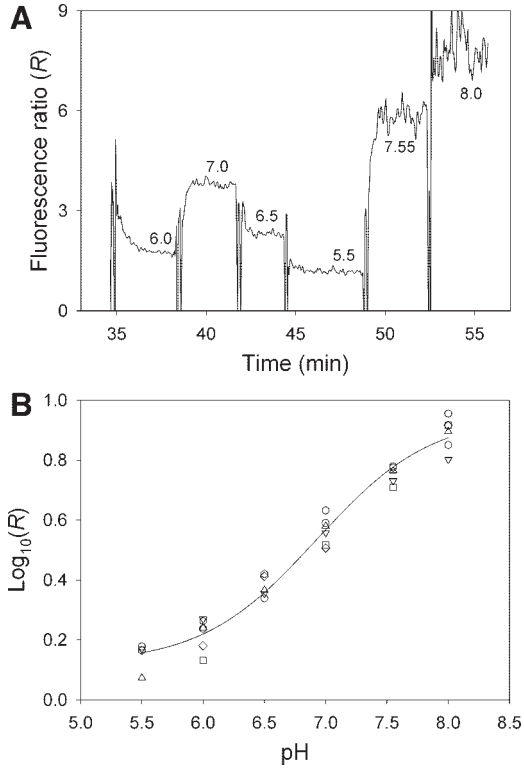

Fig. 1. *A*: calibration of the absolute pH at the end of one experiment. Intracellular pH (pH_i) values of 5.5–8.0 (indicated by the numbers) were obtained by incubating the tissue in "high" (80–100 mM) KCl solutions containing 10 μM nigericin, 2 mM $CaCl_2$, and 100 mM appropriate buffers (pH 5.5 and 6.0, MES; 6.5, bis-Tris; 7.0, BES; 7.55, HEPES; 8.0, Tricine). *B*: a fit of *Eq. 1* to data pooled from 6 experiments (represented by the different symbols) like those in *A*. A log transformation was applied to both sides of *Eq. 1* to stabilize the residual variance while preserving the functional relationship between fluorescence ratio (R) and pH. This mean calibration curve was used to calculate pH_i from R data.

and protonation of NH_3, whereas the slower decay is thought to be associated with the entry of NH_4^+, which then releases protons to the cytosol. When the pH_i had fallen to ~7, the cells were transferred to an NH_4Cl-free "recovery" solution. The ensuing efflux of NH_3 then resulted in a rapid fall in pH_i (acid load, *phase C*) followed by a slower recovery (*phase D*), presumably due to proton equivalent efflux. The recovery solution was either Ringer plus 100 μM DMA (an inhibitor of the Na^+/H^+ exchanger, Refs. 26, 28) or potassium Ringer (K-Ringer), in which NaCl is replaced by KCl (which should also prevent Na/H^+ antiport). Both solutions contained 100 nM bafilomycin A_1 to inhibit any H^+-ATPase activity (28), 100 μM SCH-28080 to inhibit any H^+/K^+-ATPase activity (24, 37), and 1 mg/ml glucose. The K-Ringer also contained 1.5 μM of the K^+ ionophore valinomycin as a precaution to ensure adequate charge compensation of electrogenic H^+ efflux. pH_o was 7.4 in Ringer and either 7.4 or 8.0 in K-Ringer; HEPES buffer was used in all solutions.

To test for Zn^{2+} sensitivity (an indication of the involvement of voltage-gated H^+ channels) the recovery solution also contained either 10 μM $ZnCl_2$ or 1 mM of the divalent cation chelator EGTA (plus an extra 1 mM $CaCl_2$ to maintain normal free Ca^{2+}). A $ZnCl_2$ concentration of 10 μM should effectively abolish any voltage-gated H^+ flux, even in cells depolarized to 0 mV (8).

During experiments, a cover glass with attached cell monolayer was held in a cover glass holder inside a spectrometer cuvette containing ~1 ml of solution, with constant stirring. We changed solutions by transferring the holder to one or two successive beakers each containing 16–18 ml of the next solution in the series and then to a cuvette containing 1 ml of that solution. When not in use, rinsing solutions were stored in an incubator at 37°C; cuvette solutions were maintained at 37°C in the spectrometer with a circulating water bath. The order of acid-load/recovery cycles with or without Zn^{2+} was varied between experiments (e.g., Fig. 3). In ~50% of experiments two acid-load/recovery cycles were achieved, and in ~10% three cycles were obtained. In the remaining experiments only a single acid-load/recovery cycle was possible because of cell loss.

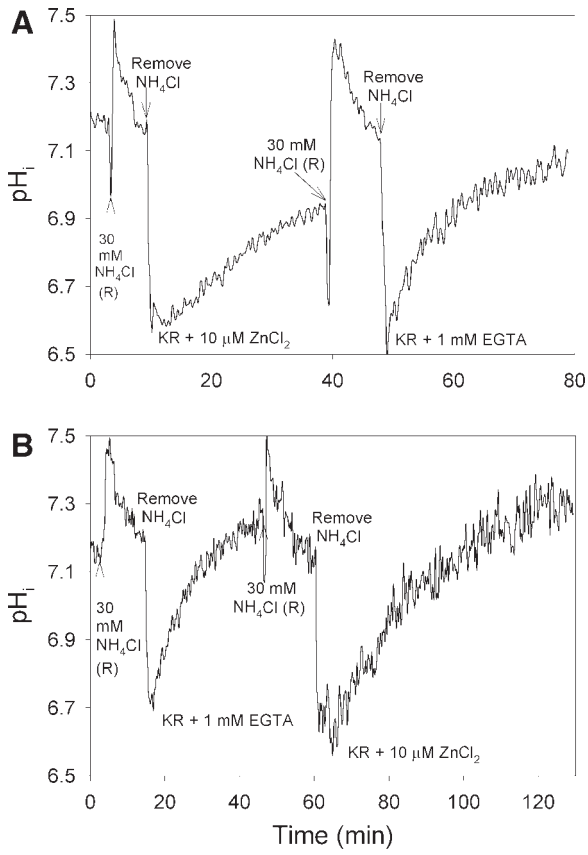

Fig. 3. Effects of Zn^{2+} on pH_i recovery at extracellular pH (pH_o) 7.4 (*A*) and pH_o 8.0 (*B*). In both we applied the NH_4Cl prepulse in Ringer (R) at pH_o 7.4 before transferring the tissue to K-Ringer (KR). Two successive acid-load/recovery cycles are shown, one with Zn^{2+}, the other without. Note that the order of the treatments is reversed in *B*. The data were smoothed with a Fourier smoother (unsmoothed data were used for curve fitting, as in Fig. 2).

Data analysis. To quantify the changes in pH_i following the removal of NH_4Cl (i.e., on transferring the cells to the recovery solution), we fitted the data for *phases C* and *D* in Fig. 2 with the following equation by nonlinear least squares (bold curve in Fig. 2)

$$pH_i(t) = pH_i(0) + \Delta pH_1(1 - e^{-t/\tau_1}) + \Delta pH_2(1 - e^{-t/\tau_2}) \quad (3)$$

where, having removed the artifact associated with the solution change, we took time $t = 0$ as midway between the end of *phase B* and the start of *phase C*. Referring to Fig. 2, data are reported in terms of t_{min} (the time to reach the pH minimum at the end of *phase C*), pH_{min} (the pH at that minimum), $\tau = \tau_2$ in *Eq. 3* (effectively the time constant of the recovery phase, *D*), and pH_{fin} (the limiting value to which the pH apparently recovers as $t \rightarrow \infty$). pH_{fin} [$= pH_i(0) + \Delta pH_1 + \Delta pH_2$] and τ ($= \tau_2$) are obtained directly from the fits of *Eq. 3*. We determined t_{min} by setting the derivative of *Eq. 3* to zero and solving for *t*. pH_{min} was then calculated by setting $t = t_{min}$ in *Eq. 3*.

In some cases the minimum was obscured by the solution-change artifact, and so the term in ΔpH_1 in *Eq. 3* was omitted. pH_{min} and t_{min} were then estimated as pH_i and *t* for the first reliable data point following the solution change (i.e., after removing the artifact). Although this is somewhat arbitrary, it was done to avoid biasing the mean value of t_{min} toward larger values. In other cases there was insufficient curvature in *phase D* for a fit of the second exponential and so it was replaced with a linear term

$$pH_i(t) = pH_i(0) + \Delta pH_1(1 - e^{-t/\tau_1}) + bt \quad (4)$$

where *b* is a constant. We again determined pH_{min} and t_{min} by setting the derivative of *Eq. 4* to zero or from the first point in *phase D* if a minimum was absent (in which case the term in ΔpH_1 was omitted); estimation of τ and pH_{fin} was not possible.

From the point of view of data analysis, the ideal experiment is like those shown in Fig. 3, in which Zn^{2+} and control (EGTA) data are available in the same experiment. If the data from control and Zn^{2+}-exposed cells are correlated, the use of such paired data will improve the precision of parameter-ratio estimates and hence increase the power of statistical tests. Paired data were analyzed as described in RESULTS. However, to limit the analysis to paired data would be to discard about one-third of the experiments. Hence, if paired data are not correlated it is better to use all the data (paired and unpaired) and so increase the sample size. For recovery in Ringer at a single pH_o (7.4) this is easily achieved with one-way analysis of variance (ANOVA). For recovery in K-Ringer at two different pH_o (7.4 and 8.0), the following model was fitted to all the data by least squares

$$x = \mu \quad (pH_o = 7.4, [Zn^{2+}] = 0) \quad (5a)$$

$$x = \alpha\mu \quad (pH_o = 7.4, [Zn^{2+}] > 0) \quad (5b)$$

$$x = \beta\mu \quad (pH_o = 8.0, [Zn^{2+}] = 0) \quad (5c)$$

$$x = \alpha\beta\gamma\mu \quad (pH_o = 8.0, [Zn^{2+}] > 0) \quad (5d)$$

where *x* represents t_{min}, pH_{min}, τ, or pH_{fin}; μ is the value of *x* when $pH_o = 7.4$ and $[Zn^{2+}] = 0$; α is the factor by which *x* is changed by Zn^{2+} at $pH_o = 7.4$; β is the factor by which *x* is changed by a change in pH_o (7.4 → 8.0) when $[Zn^{2+}] = 0$; and γ allows for the possibility that the effect of Zn^{2+} is different at different pH_o, and vice versa (if there is no such interaction between the effects of Zn^{2+} and pH_o, then $x = \alpha\beta\mu$ when $pH_o = 8.0$ and $[Zn^{2+}] > 0$). Various reduced models were then fitted by setting α, β, or γ to unity. A minimum-parameter model was chosen by using *F* tests at the 5% significance level as described by Walpole and Myers (40). Specifically, for two models

with k and $k - 1$ parameters (e.g., for $k = 4$, models with parameters $\mu, \alpha, \beta, \gamma$ and μ, α, β) an F value with $(1, n - k)$ degrees of freedom (where n is the number of x values) was calculated as

$$F = \frac{RSS_{k-1} - RSS_k}{RSS_k/(n-k)} \quad (6)$$

where RSS is the residual sum of squares. If the F value was significant the k-parameter model was retained, otherwise it was rejected in favor of the reduced model with $k - 1$ parameters. When nonsignificant F values were obtained with more than one reduced model, the one with the smallest RSS_{k-1} was chosen for the next round of F tests (i.e., against models with $k - 2$ parameters).

As judged by t-tests at the 5% level and visual inspection of the data, there was no evidence that the order of the applied treatments (i.e., $Zn^{2+} \rightarrow$ EGTA or EGTA $\rightarrow Zn^{2+}$) affected x, and so order does not appear as a factor in *Eq. 5, a–d*. Rather, for all types of analysis (paired, ANOVA, and *Eq. 5, a–d*), control data obtained before and after the Zn^{2+} treatment were pooled, as were the Zn^{2+} data obtained before and after the EGTA treatments. (In this case the ANOVA is equivalent to a two-sample t-test; Ref. 40) For t_{min} and τ, a log transformation was applied to both sides of *Eq. 5, a–d*, to stabilize the variance and reduce positive skew; this was not necessary for pH_{min} and pH_{fin} (presumably because these variables are already log-transformed). Mean values are given with standard errors and, where appropriate, the number of observations in parenthesis. A significance level of 0.05 was used for all statistical tests.

Boyarsky et al. (4) concluded that in a variety of cells at around pH_i 7, the high K^+/nigericin calibration technique led to estimates of pH_i ($pH_{i,nig}$) that were 0.08–0.26 pH units above the true pH_i ($pH_{i,true}$). At least part of the error probably arose because $[K^+]$ in the calibration solutions was too low; this was likely true in the present study also. In a subsequent paper on smooth muscle cells, Boyarsky et al. (5) found that the error varied from ~0 to ~0.3 pH units over the $pH_{i,nig}$ range 6–8. Furthermore, the error increased approximately linearly with $pH_{i,nig}$ such that

$$pH_{i,nig} - pH_{i,true} = A + B pH_{i,nig} \quad (7)$$

where A and B are constants. As pointed out by Boyarsky et al. (5), such a linear relationship will mean that t-tests on pH_i values are unaffected. The same can be said of F-tests; the RSS values in the numerator and denominator of *Eq. 6* are simply multiplied by $(1 - B)^2$ (40) so that the F values are unaffected. Hence, assuming any error in the present study was also linearly related to $pH_{i,nig}$, the conclusions regarding pH_{min} and pH_{fin} are unaltered, even though the absolute values of pH_{min} and pH_{fin} may be in error. As regards t_{min} and τ, it is readily shown from *Eqs. 3* and *7* that estimates of these parameters are unaffected by a linear transformation in $pH_{i,nig}$.

Mathematical and statistical analyses were carried out with Mathematica v. 4.2 (Wolfram Research, Champaign, IL), the NAG Fortran Library Mark 20 (Numerical Algorithms Group, Downers Grove, IL) running under Compaq Visual Fortran v. 6.6 (Compaq Computer, Houston, TX), and with software written in True BASIC Gold Edition (True BASIC, Hartford, VT).

RESULTS

Resting pH_i in Ringer solution. At the beginning of each experiment the cells were placed in Ringer solution (pH 7.4) and a baseline pH_i was established. The average pH_i was 7.13 ± 0.17 (mean ± SD, $n = 38$). The average pH_i measured in Ringer solution after recovery from the first acid load (pH_{fin}) was not significantly different, 7.04 ± 0.06 (means ± SE, $n = 11$), indicating little drift during the 30- to 50-min experiments. After recovery in K-Ringer, average pH_i was identical to that in Ringer, 7.00 ± 0.05 (means ± SE, $n = 13$).

To test whether proton channels help maintain the resting pH_i in rat alveolar epithelial cells, we added 100 μM $ZnCl_2$ to the Ringer solution (without EGTA) and measured pH_i for 20–30 min. As illustrated in Fig. 4, there was no discernable effect. Similar results were obtained in three experiments. We routinely employ EGTA (with added $CaCl_2$ to maintain normal free Ca^{2+}) to eliminate polyvalent metal contaminants. Therefore, in three analogous experiments, Ringer with EGTA was used as the control solution before and after exposure to 10 μM $ZnCl_2$ (no EGTA in the $ZnCl_2$ solution). Again, no effect on pH_i could be detected. After testing for effects of $ZnCl_2$, we added NH_4^+ to verify that the cells were still viable and responsive. Evidently, proton channels are not open under resting conditions.

pH_i recovery in K-Ringer. Most experiments were done in high-$[K^+]$ solution, K-Ringer, both to prevent Na^+/H^+-antiport and to depolarize the cells and thereby promote opening of voltage-gated H^+ channels. Cells in normal Ringer solution are expected to maintain a more negative membrane potential, which should lower H^+ channel open probability. Experiments were done at both pH_o 7.4 and pH_o 8.0, because high pH_o promotes H^+ channel opening (10). Figure 3 shows that at both pH_o 7.4 (Fig. 3*A*) and pH_o 8 (Fig. 3*B*), 10 μM Zn^{2+} slowed pH_i recovery following an acid load and also appeared to delay the onset of recovery. In experiments such as these, the changes in pH_i following removal of NH_4^+ were quantified by the parameters t_{min}, τ, pH_{min}, and pH_{fin}, as illustrated in Fig. 2. Often it was possible to estimate these parameters in the presence and absence of Zn^{2+} within a single experiment (Fig. 3), although sometimes cell detachment meant that only a single acid-load/recovery cycle was obtained (i.e., either Zn^{2+} or EGTA, but not both in the same experiment).

Mean values of t_{min}, τ, pH_{min}, and pH_{fin} before, during, and after the Zn^{2+} treatment are summarized in Fig. 5. (The "Before" and "After" solutions contained 1 mM EGTA, and so Zn^{2+} should have been essentially absent.) In considering these mean values, we find the overall impression to be that Zn^{2+} slows recovery (i.e., increases t_{min} and τ; Fig. 5, *A* and *B*) but does not reduce the final level of recovery (pH_{fin}, Fig. 5*D*). Also the acid load itself is more extreme (i.e., pH_{min} is lower;

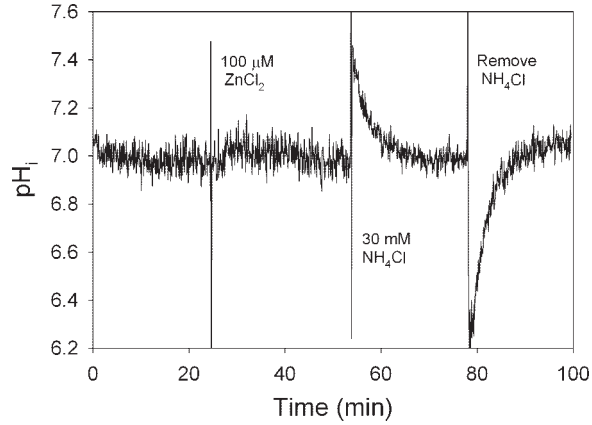

Fig. 4. Lack of effect of 100 μM $ZnCl_2$ on pH_i in unchallenged alveolar epithelial cells bathed in Ringer solution. At ~24 min into the experiment, 10 μl of 10 mM $ZnCl_2$ in water was added to the cuvette to give a final concentration of 100 μM. Later, we introduced and then removed 30 mM NH_4^+ (by transferring the tissue to NH_4Cl-free Ringer), resulting in normal pH_i changes, like those described in Fig. 2.

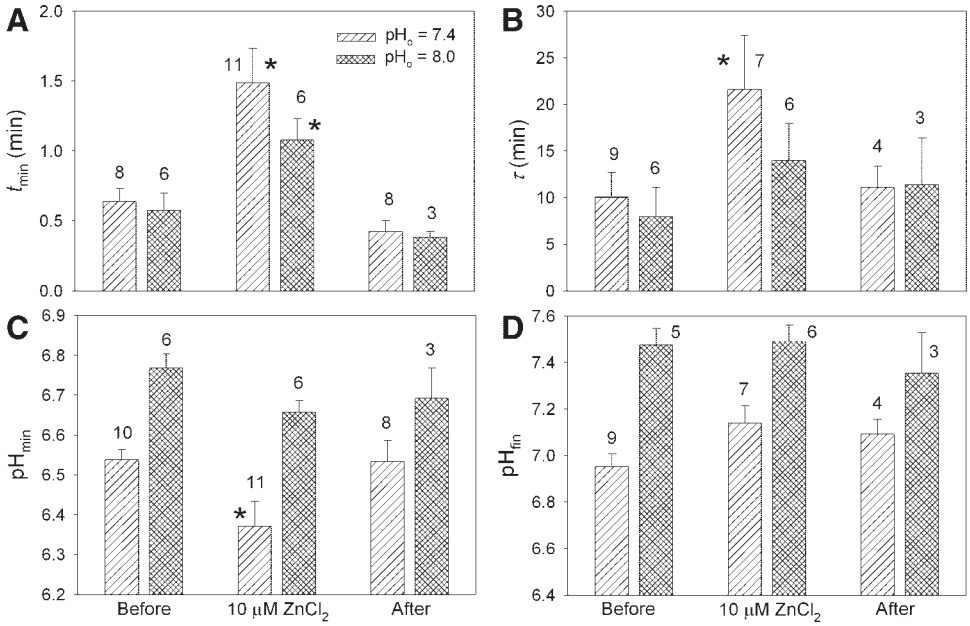

Fig. 5. Mean values of t_{min}, τ, pH_{min}, and pH_{fin} for pH_i recovery in K-Ringer in the presence and absence of Zn^{2+} (see Fig. 2 for the meaning of these parameters). Statistical analyses (Table 1 and Fig. 6) showed that Zn^{2+} significantly increased t_{min} and τ (*A* and *B*) and significantly reduced pH_{min} (*C*). Zn^{2+} had no significant effect on pH_{fin} (*D*). Zn^{2+} solutions contained 10 μM $ZnCl_2$, whereas Zn^{2+}-free solutions ("Before" and "After") contained 1 mM EGTA. The numbers above each bar show the number of observations; error bars are standard errors; *significant differences at a given pH_o in the presence and absence of Zn^{2+}.

Fig. 5*C*) in the presence of Zn^{2+}. These effects of Zn^{2+} were reversible (compare Fig. 3, *A* and *B*, as well as the Before and After mean values in Fig. 5). To test the statistical significance of these apparent effects, we subjected the data to the model-selection procedure described in the MATERIALS AND METHODS (*Eq. 5, a–d*). This analysis, which is summarized in Table 1, essentially confirms one's subjective impression of the data. Thus Zn^{2+} produced an approximately twofold increase in t_{min} and τ at both pH_o (Fig. 5, *A* and *B*). Although the τ data at pH_o 8.0 in Fig. 5*B* are fitted almost as well by a model in which there is no effect of Zn^{2+} (the effect at pH_o 7.4 is significant), this was evidently due to variability in the control τ values, as can be seen in Fig. 6. If we select those experiments (e.g., Fig. 3) in which pH recovery time constants both in the presence and absence of Zn^{2+} (τ_{Zn} and τ_{EGTA}, respectively) were obtained in the same experiment, then a clear effect of Zn^{2+} at pH_o 8.0 emerges. For these paired data, τ_{Zn} and τ_{EGTA} were significantly correlated (Fig. 6), which means that the errors on estimates of τ_{Zn}/τ_{EGTA} can be reduced relative to those obtained from unpaired data. Estimates of τ_{Zn}/τ_{EGTA} obtained from paired data were significantly greater than unity at both pH_o 7.4 (2.34 ± 0.36, $n = 4$) and pH_o 8.0 (2.52 ± 0.40, $n = 5$).

The statistical analysis also confirmed that pH_{min} is reduced in the presence of Zn^{2+}, at least at pH_o 7.4, and there was a clear effect of pH_o, such that pH_{min} was higher at pH_o 8.0 than at pH_o 7.4 (Fig. 5*C*). There was no statistically significant effect of Zn^{2+} on pH_{fin}, i.e., pH_i recovered to about the same level in the presence or absence of Zn^{2+} (albeit over a longer time course in the presence of Zn^{2+}). As one might expect, pH_{fin} was significantly higher at pH_o 8.0 than at pH_o 7.4 (Fig. 5*D*).

The outcome of statistical analysis of the effects of Zn^{2+} and pH_o on acid loading and pH_i recovery is illustrated by the

Table 1. *Results of the statistical analysis to determine the effects of Zn^{2+} and pH_o on t_{min}, τ, pH_{min} and pH_{fin} for tissue in K-Ringer*

x	μ	α	β	γ
t_{min}, min	0.462±0.052	2.51±0.45	1	1
τ, min	7.9±1.1	1.87±0.43	1	1
pH_{min}	6.524±0.030	0.9793±0.0064	1.0368±0.0069	1
pH_{fin}	7.045±0.040	1	1.0582±0.0095	1

Data in Fig. 5 were fitted with *Eq. 5, a–d*, as well as various reduced models obtained by setting α, β, or γ to unity. "Before" and "After" data were pooled. The best-fit, minimum-parameter models were chosen by *F*-tests at the 5% level. The table gives the parameter estimates for these models with SE. μ is the value of *x* when extracellular pH (pH_o) = 7.4 and $[Zn^{2+}] = 0$, α is the factor by which *x* is changed by Zn^{2+} at $pH_o = 7.4$, β is the factor by which *x* is changed by a change in pH_o (7.4 → 8.0) when $[Zn^{2+}] = 0$, and γ allows for the possibility that the effect of Zn^{2+} is different at different pH_o (and vice versa). A value of unity for α or β implies no effect of Zn^{2+} or pH_o, respectively. Since γ was always unity, there was no interaction between the effects of Zn^{2+} and pH_o (i.e. the value of *x* when $pH_o = 8.0$ and $[Zn^{2+}] > 0$ is simply μαβ). pH_{fin}, limiting value to which the pH apparently recovers as $t \rightarrow \infty$; t_{min}, the time to reach the pH minimum at the end of *phase C;* pH_{min}, pH at that minimum; τ, time constant of pH_i recovery.

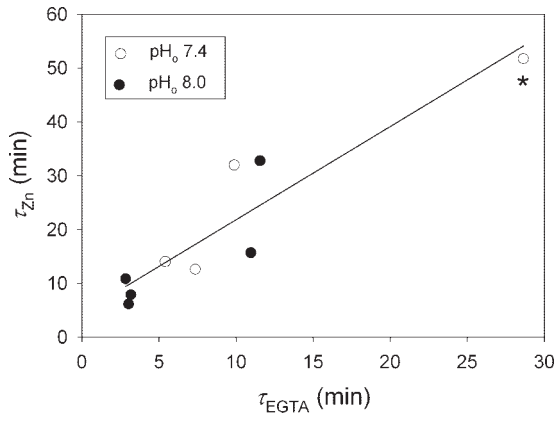

Fig. 6. The pH_i recovery time constants in the presence and absence of Zn^{2+} (τ_{Zn} and τ_{EGTA}, respectively) were significantly correlated ($P < 0.001$). The correlation is still significant if the extreme point (*) is omitted ($P < 0.02$). Each point represents a different experiment. The mean ratios τ_{Zn}/τ_{EGTA} were 2.34 ± 0.36 and 2.52 ± 0.40 for pH_o 7.4 and 8.0, respectively (both significantly greater then unity). Pooling the data for both pH_o gave a value 2.44 ± 0.26.

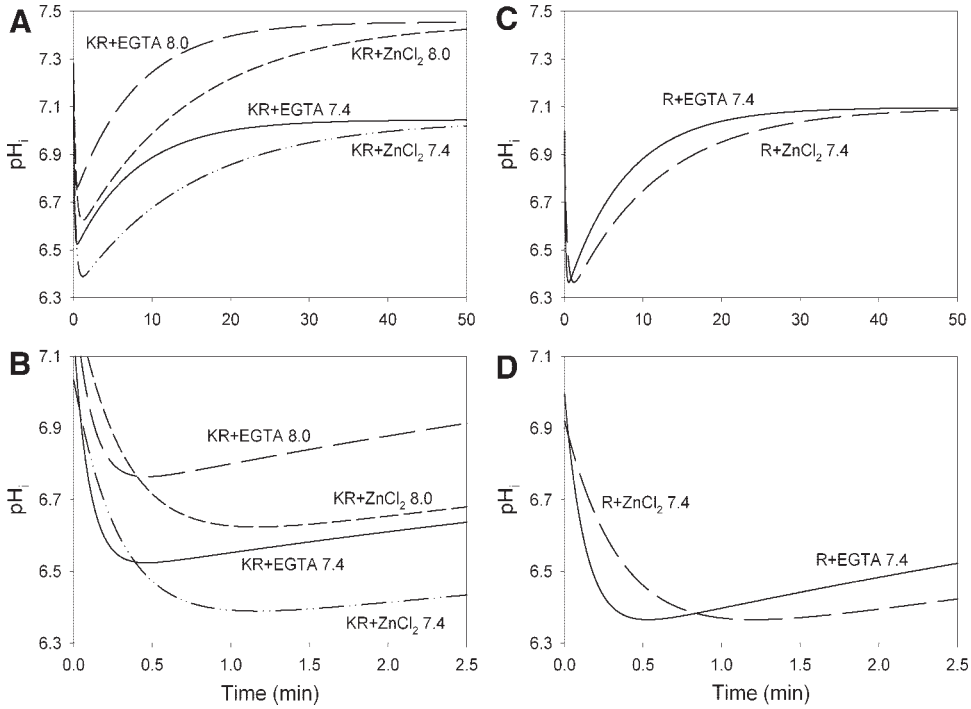

Fig. 7. Idealized pH_i recovery time courses reconstructed statistically from all of the experimental data. *A* and *B*: plots of pH_i vs. *t* predicted by the best-fit models in Table 1. To produce these plots, we generated predicted mean values of t_{min}, τ, pH_{min}, and pH_{fin} by substituting the parameter values from Table 1 into *Eq. 5, a–d*. Using these values, expressions for t_{min}, pH_{min}, and pH_{fin} derived from *Eq. 3* were then solved simultaneously for τ_1, ΔpH_1, and ΔpH_2, and τ_2 was set equal to τ. Finally, pH(0) was set to its mean value, and the curves in *A* and *B* were generated with *Eq. 3*. The curves in *A* illustrate how Zn^{2+} caused a similar relative slowing of recovery (increase in τ) in K-Ringer at both pH_o (7.4 and 8.0) but had no significant effect on the final level of pH recovery (pH_{fin}). In *B* the early portions of the curves in *A* are shown on an expanded time scale. The increased acid load (lower pH_{min}) and delayed recovery (larger t_{min}) in the presence of Zn^{2+} are evident. *C* and *D*: similar plots for recovery in Ringer (pH_o 7.4); for these plots pH(0) was set to its mean value and the values of t_{min}, τ, pH_{min}, and pH_{fin} were taken from Fig. 10 ("Before" and "After" data were pooled).

graphs in Fig. 7, *A* and *B*, which shows plots of pH_i vs. *t* predicted by the best-fit models in Table 1 (see Fig. 7 legend for details). The curves in Fig. 7*A* illustrate that Zn^{2+} caused a similar relative slowing of recovery (increase in τ) at both pH_o 7.4 and pH_o 8.0 but had no significant effect on the final level of pH recovery (pH_{fin}). In Fig. 7*B* the early portions of the curves in Fig. 7*A* are shown on an expanded time scale. The increased acid load (lower pH_{min}) and delayed recovery (larger t_{min}) in the presence of Zn^{2+} are evident.

Maximum H^+ fluxes in K-Ringer. The curves in Fig. 7*A* allow us to calculate a quantity qJ_H (Fig. 8) that is proportional to the Zn^{2+}-sensitive H^+ flux (J_H), which we attribute to H^+ transport through voltage-gated proton channels (*q* is the apical surface area to volume ratio of the monolayer ≈1/monolayer thickness). qJ_H was calculated as

$$qJ_H = B_i\left(\frac{dpH_i}{dt}\right)_{Zn} - B_i\left(\frac{dpH_i}{dt}\right)_{EGTA} \quad (8)$$

where $(dpH_i/dt)_{Zn}$ and $(dpH_i/dt)_{EGTA}$ are the rates of change of pH_i in the presence and absence of Zn^{2+} respectively, and B_i is the (pH_i-dependent) intracellular buffer capacity. In this formulation, proton efflux is a negative quantity. To employ *Eq. 8*, $(dpH_i/dt)_{Zn}$ and $(dpH_i/dt)_{EGTA}$ were determined at the same pH_i, and calculations were restricted to times $t > 3\tau_1$ (see *Eq. 3*) so as to be clear of the pH_i minimum (so that changes in pH_i reflect J_H rather than NH_3 and NH_4^+ fluxes). Values of B_i were taken from Fig. 1 in Lubman and Crandall (26). Although these values pertain to 22°C rather than 37°C, we are really only seeking an order of magnitude calculation here. In Fig. 8 qJ_H is plotted against pH_i (solid curves). It can be seen that at both pH_o, the maximum qJ_H approaches 2 mM/min. If one assumes a monolayer thickness of 1–5 μm (i.e., q = 0.2–1/μm), this implies a maximum equivalent proton-current density across the apical membrane of 3–16 fA/μm^2. This calculation assumes that *1*) the J_H observed in the presence of Zn^{2+} persists unaltered and simply adds to J_H when Zn^{2+} is removed and *2*) the rate of production of H^+ by metabolism is the same in the presence and absence of Zn^{2+}.

Boyarsky et al. (4, 5) concluded that the high K^+/nigericin calibration technique leads to overestimates of pH_i. As discussed in the MATERIALS AND METHODS, this error does not affect the conclusions regarding t_{min}, τ, pH_{min}, and pH_{fin} but would affect the estimates of qJ_H. From Boyarsky et al. (5) the true value of qJ_H is given by

$$qJ_{H,true} = qJ_{H,nig}\, 10^{pH_{error}} \quad (9)$$

where $qJ_{H,nig}$ is the value of qJ_H calculated under the assumption that the high-K^+/nigericin calibration technique is unbiased, and pH_{error} is the amount by which pH_i is overestimated. Assuming pH_{error} = 0.0–0.3 (5), the calculated maximum

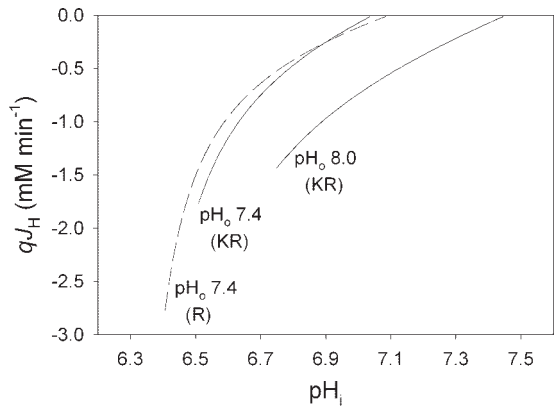

Fig. 8. The quantity qJ_H was calculated from the curves in Fig. 7, *A* and *C*, according to *Eq. 8*. J_H is the Zn^{2+}-sensitive transapical membrane H^+ efflux (considered negative), and *q* is the apical surface area to volume ratio (≈1/monolayer thickness). Calculations were restricted to times $t > 3\tau_1$ to ensure that dpH_i/dt reflects mainly the proton efflux. KR, solid curves; R, dashed curve.

current density should be increased by a factor of 1–2. So instead of 3–16 fA/μm^2 as calculated above, a reasonable range might be 3–30 fA/μm^2. Assuming a membrane capacitance of 1 $\mu F/cm^2$, we can translate this to a normalized H^+ current (I_H) = 0.3–3 pA/pF. As a frame of reference, I_H is typically 10–20 pA/pF during large depolarizations in rat alveolar epithelial cells over a wide pH range (9). The I_H required to produce the pH_i recovery in this study thus requires activating only a small fraction of the maximum available H^+ conductance.

SCH-28080, bafilomycin A_1, Zn^{2+}, and 4,4′-dibenzamidostilbene-2,2′-disulfonic acid did not prevent pH_i recovery in K-Ringer. As a precaution, we routinely included 100 μM SCH-28080 in the K-Ringer recovery solutions to inhibit any H^+/K^+-ATPase activity (37). In a subset of experiments this inhibitor was omitted. No effect of SCH-28080 was detected (Table 2), suggesting an absence of H^+/K^+-ATPase activity in rat alveolar epithelial cells. This corroborates the results of Kemp et al. (24), who found evidence for an H^+/K^+-ATPase in type II pneumocytes of guinea pig but not those of rat. The K-Ringer also contained 100 nM bafilomycin A_1, a specific inhibitor of V-type H^+-ATPases. Despite the presence of 100 nM bafilomycin A_1, 10 μM $ZnCl_2$, and no external Na^+ (hence no Na^+/H^+ exchange), pH_i recovery still occurred following an acid load. As pointed out by Richard D. Vaughan-Jones (personal communication), the presumed membrane depolarization in K-Ringer would lead to an accumulation of intracellular Cl^-, which might then result in pH_i recovery via Cl^-/OH^- exchange. To test whether this mechanism might contribute under the present conditions, we conducted a separate set of experiments with the anion-transporter inhibitor 4,4′-dibenzamidostilbene-2,2′-disulfonic acid (DBDS, Ref. 38). Adding 0.2 mM DBDS to the recovery solution containing all other inhibitors (K-Ringer containing 100 nM bafilomycin A_1, 100 μM SCH-28080, 10 μM $ZnCl_2$, and 1.5 μM valinomycin) had no significant effect on pH_i recovery (Table 3). Given the variability of the data, we cannot exclude a small effect, but it is clear that cells still recovered from an acid load in the presence of DBDS. Hence the residual pH_i recovery is apparently not primarily associated with a DBDS-sensitive anion transporter.

pH_i recovery in Ringer with normal $[K^+]_o$. To test the possibility that the residual (Zn^{2+}-insensitive) pH_i recovery was associated with elevated external K^+ (e.g., a K^+/H^+ exchanger; Ref. 2), we conducted experiments in Ringer (pH_o 7.4) using 100 μM DMA to block the Na^+/H^+ exchanger (26, 28). The Ringer solution also contained 100 nM bafilomycin A_1 and 100 μM SCH-28080 (but no valinomycin). It was also of interest to examine the effects of 10 μM $ZnCl_2$ in this more physiological medium. If the resting membrane potential were more negative in Ringer, this would be expected to decrease Zn^{2+}-sensitive J_H via voltage-gated H^+ channels (9). As usual, Zn^{2+}-free Ringer contained 1 mM EGTA plus an additional 1 mM $CaCl_2$. Fig. 9 shows example pH_i records with $ZnCl_2$ applied before (Fig. 9*A*) or after (Fig. 9*B*) the EGTA control. Surprisingly, 10 μM Zn^{2+} slowed recovery in Ringer solution. As in K-Ringer, recovery still occurred in Ringer despite addition of the entire gamut of inhibitors.

Table 2. *H^+/K^+-ATPase inhibitor SCH-28080 had no detectable effect on τ or pH_{fin} in the absence of Zn^{2+}, or on pH_{min}*

Parameter	$[Zn^{2+}]$, μM	SCH-28080	
		100 μM	0 μM
τ, min	0	6.64±0.67 (7)	7.83±0.26 (3)
pH_{fin}	0	7.004±0.062 (8)	6.91±0.10 (3)
pH_{min}	0	6.590±0.035 (10)	6.505±0.072 (5)
pH_{min}	10	6.355±0.077 (7)	6.44±0.10 (5)

The data were insufficient and/or too variable for a meaningful analysis of other parameters (τ in the presence of Zn^{2+}, t_{min}, etc.). Mean values are given with SE and the number of observations in parenthesis.

Table 3. *Anion-transport inhibitor DBDS had no detectable effect on pH_i recovery following an NH_4Cl prepulse*

Parameter	DBDS	
	0.2 mM	0 mM
t_{min}, min	1.09±0.54 (5)	1.08±0.15 (6)
τ, min	10.8±3.4 (5)	14.0±4.0 (6)
pH_{min}	6.40±0.11 (4)	6.657±0.029 (6)
pH_{fin}	7.60±0.13 (4)	7.490±0.069 (6)

pH_i recovery was monitored in K-Ringer (pH_o 8) containing 100 nM bafilomycin A_1, 100 μM SCH-28080, 10 μM $ZnCl_2$, and 1.5 μM valinomycin. Mean values are given with SE and the number of observations in parenthesis. DBDS, 4,4′-dibenzamidostilbene-2,2′-disulfonic acid; pH_i, intracellular pH; K-Ringer, potassium Ringer solution.

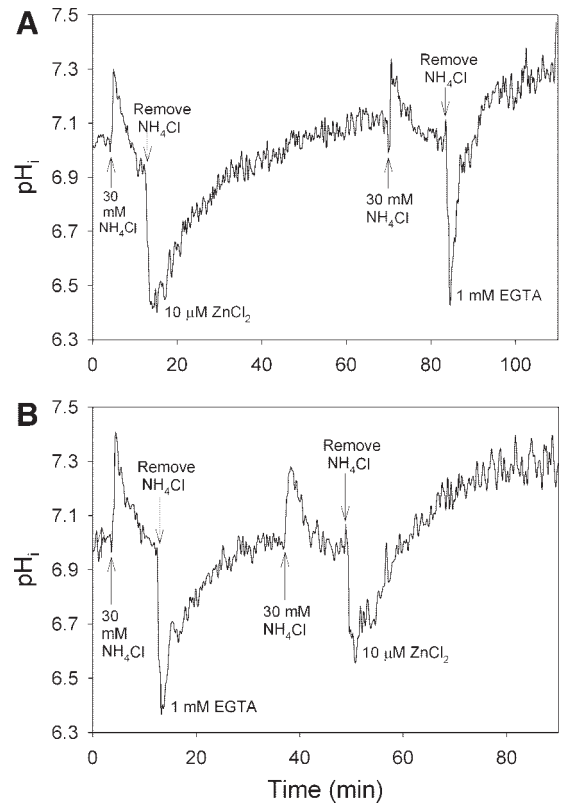

Fig. 9. Two experiments (*A* and *B*) in which the tissue was bathed in Ringer (pH_o 7.4) containing 0.1 mM 5-(*N,N*-dimethyl)amiloride (DMA), 0.1 μM bafilomycin A_1, and 0.1 mM SCH-28080. In both cases, 2 successive acid-load/recovery cycles were achieved, one with Zn^{2+}, the other without. The order of the treatments is reversed in *B*. The data were smoothed with a Fourier smoother (unsmoothed data were used for curve fitting, as in Fig. 2).

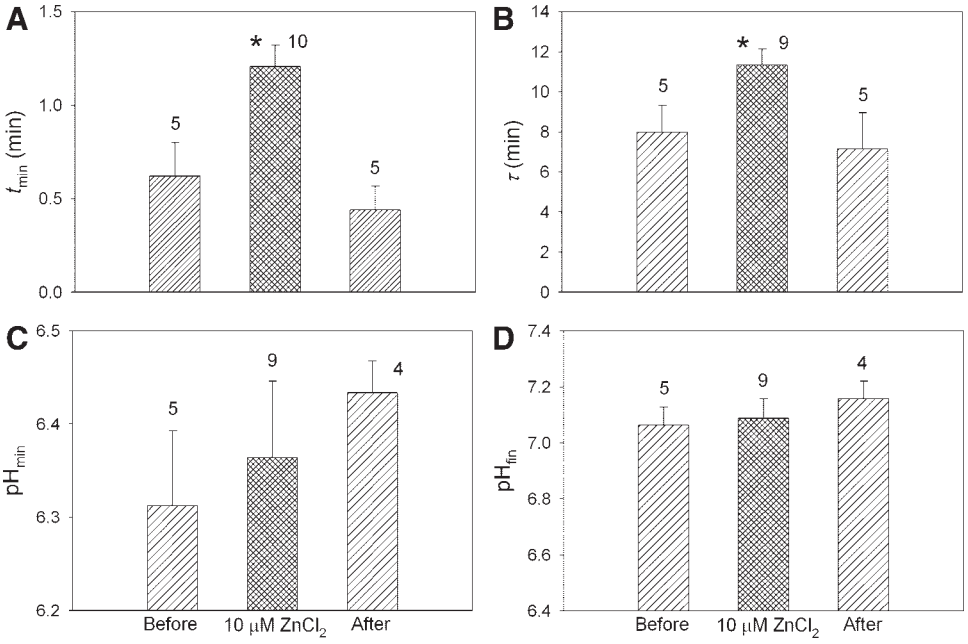

Fig. 10. Mean values of t_{min}, τ, pH_{min}, and pH_{fin} in the presence and absence of Zn^{2+} for tissue bathed in Ringer plus 0.1 mM DMA, 0.1 μM bafilomycin A_1, and 0.1 mM SCH-28080. One-way ANOVA showed that Zn^{2+} significantly increased t_{min} and τ (* in *A* and *B*) but had no significant effect on pH_{min} and pH_{fin} (*C* and *D*). However, large standard errors on at least 2 of the pH_{min} estimates may have precluded detection of a Zn^{2+} effect (*C*). Zn^{2+} solutions contained 10 μM $ZnCl_2$ while Zn^{2+}-free solutions (Before and After) contained 1 mM EGTA. The numbers above each bar show the number of observations; error bars are standard errors.

Figure 10 summarizes the mean values of t_{min}, τ, pH_{min}, and pH_{fin} for experiments in Ringer solution. As with the K-Ringer data, these mean values were used to generate the pH(*t*) plots in Fig. 7, *C* and *D*, and the qJ_H plot (dashed curve) in Fig. 8 (see legends to Figs. 7 and 8 for details). The overall impression is that recovery in Ringer is generally similar to recovery in K-Ringer at pH_o 7.4, both in kinetics and effects of Zn^{2+} (compare Figs. 5 and 10; Fig. 7, *A*, *B* and *C*, *D*, and the pH_o 7.4 curves in Fig. 8). One difference was that Zn^{2+} had no detectable effect on pH_{min} in Ringer. As with K-Ringer, there was no effect of Zn^{2+} on pH_{fin} (Fig. 10*D*). One-way ANOVA, as well as analysis of paired data, shows that Zn^{2+} significantly increased both t_{min} (Fig. 10*A*) and τ (Fig. 10*B*), although the slowing of τ was less profound than in K-Ringer. In summary, the effects of Zn^{2+} were less pronounced in normal-Na^+ Ringer solution, but both the Zn^{2+}-sensitive and Zn^{2+}-insensitive components of pH_i recovery following an acid load still occurred.

DISCUSSION

pH_i in unchallenged alveolar epithelial cells. The average baseline pH_i was 7.13, within the lower range of values in previous studies of cultured rat alveolar type II epithelial cells in nominally HCO_3^--free solutions, 7.17–7.36 (6, 19, 36); a higher value of 7.50 has also been reported (25, 28).

Given the strong regulation of their gating by pH, one would predict that proton channels would not be open under resting conditions. Voltage-gated proton channels open only positive to the Nernst potential for H^+ (E_H) (9, 11), with the result that they always extrude acid. Because E_H is normally positive to the resting membrane potential in alveolar epithelial cells (10), proton channels would be expected to be closed in an unchallenged cell. The data confirm this expectation. Addition of 10–100 μM $ZnCl_2$ had no effect on the baseline pH_i. Although a variety of alternative explanations could be suggested, the simplest interpretation is that proton channels are not open under resting conditions.

Zn^{2+}-sensitive pH_i recovery: voltage-gated proton channels. Several types of evidence support the conclusion that voltage-gated proton channels contribute to pH_i recovery after acid loading of rat alveolar epithelial cells. In Ringer and K-Ringer, respectively, pH_i recovery was slowed on average 1.50-fold and 2.44-fold by the addition of 10 μM $ZnCl_2$ (Figs. 5*B*, 6, and 10*B*). Although Zn^{2+} has effects on many proteins, including many ion channels, it is a potent inhibitor of voltage-gated proton channels. At pH ≥7, 10 μM Zn^{2+} severely inhibits proton currents (8) but has relatively little effect on several other ion channels (11), including voltage-gated K^+ channels in type II cells (V. V. Cherny and T. E. DeCoursey, unpublished) and cGMP-activated cation channels in type II cells (23). We thus attribute the slowing of pH_i recovery by $ZnCl_2$ to inhibition of proton channels. These effects of Zn^{2+} were observed under conditions designed to prevent the operation of other pH regulating transporters. Two more subtle effects of Zn^{2+} also suggest the involvement of the proton conductance. The time to reach the pH_i nadir (t_{min}) increased (Figs. 5A and 10*A*), and, at least in K-Ringer, pH_{min} was lower in the presence of Zn^{2+} (Fig. 5*C*). Both of these effects indicate that the proton conductance was activated rapidly, before t_{min} was reached. The effects of Zn^{2+} were reversible; *t*-tests on parameter estimates obtained before and after treatment with Zn^{2+} were never significant. Finally, the H^+ efflux was substantially larger at a given pH_i when pH_o was 8.0 than 7.4 (Fig. 8), which is consistent with the well-established pH_o dependence of proton channels (9, 11). A qualitatively similar effect of pH_o would also be expected for any transporter that is driven by the pH gradient. In summary, the data strongly support the interpretation that the Zn^{2+}-inhibitable component of pH_i recovery is mediated by voltage-gated proton channels.

Zn^{2+} had no significant effect on pH_{fin} (Figs. 5*D* and 10*D*). That is, although Zn^{2+} slowed recovery, it did not alter the final level of recovery. This is not surprising given the effects of transmembrane pH gradients on H^+ channel gating and the lack of effect of Zn^{2+} on unchallenged cells (Fig. 4). H^+

channels open only at membrane potentials positive to E_H, and the threshold voltage ($V_{threshold}$) for opening is described by the following empirical relation (9)

$$V_{threshold}(mV) = 20 - 40\Delta pH, \quad (10)$$

where $\Delta pH = pH_o - pH_i$. For the K-Ringer experiments in the absence of Zn^{2+}, pH_{fin} was 7.040 ± 0.040 ($n = 21$) and 7.456 ± 0.051 ($n = 14$) at pH_o 7.4 and 8.0, respectively. So on setting $pH_i = pH_{fin}$, *Eq. 10* gives $V_{threshold}$ values of 5.6 mV and −1.8 mV at pH_o 7.4 and 8.0, respectively. Thus at pH_{fin} and if it is assumed the cells were depolarized to near zero, any contribution of voltage-gated proton channels to H^+ efflux will be small, even in the absence of Zn^{2+}. In other words, as H^+ efflux increases pH_i, the resulting dissipation of the pH gradient shuts off the proton conductance. Accordingly, pH_{fin} will be determined mainly by any Zn^{2+}-insensitive H^+ transport and the rate of production of H^+ by metabolism. For the same reasons, proton channels do not contribute to pH_i in resting, unchallenged cells (Fig. 4); Zn^{2+} did not change baseline pH_i in cells in Ringer solution. Proton channels are expected to come into play when cells are challenged by periods of intense metabolic activity, membrane depolarization, acid loading, or other stressful conditions. Thus we cannot blithely extend the conclusion regarding proton channel activity to the in vivo situation, because the environment of cultured alveolar epithelial cells in these experiments differs radically from that in vivo, in which there is continuous CO_2 flux as well as a large pH gradient across the epithelium.

The Zn^{2+}-sensitive component of pH_i recovery (Fig. 8) represents proton currents of ~0.3–3 pA/pF or less. Is this flux consistent with known properties and magnitude of the voltage-gated proton conductance? From whole cell patch-clamp studies, the expected normalized I_H is given to a first approximation by

$$I_H = \frac{G_{H,max}(V + 2.303RT\Delta pH/F)}{1 + \exp[(a + b\Delta pH - V)/V_s]} \quad (11)$$

where V is the membrane potential, R is the universal gas constant, T is the absolute temperature, F is Faraday's constant, $a \approx 40$ mV, $b \approx -40$ mV/pH, the slope factor $V_s \approx 10$ mV, and the normalized maximum H^+ conductance ($G_{H,max}$) is ~100 pS/pF at 20°C (9). $G_{H,max}$ at 37°C is at least 3.5 times larger (14). Assuming $\Delta pH \approx 1$ and $V = 0$ in K-Ringer, *Eq. 11* predicts a proton current, $I_H \approx RTG_{H,max}/F \approx 10$ pA/pF, under "typical" conditions at the peak of the experimental acid load. The Zn^{2+}-sensitive I_H calculated above from the observed rate of pH_i change (Fig. 8) is smaller than this value. However, it is necessary to consider the dynamic nature of events during the acid load and recovery processes. Before the acid load, the K^+ conductance may successfully clamp the membrane potential near 0 mV. However, when pH_i drops to pH_{min}, E_H will shift to −53 mV (for pH_o 7.4) or −77 mV (for pH_o 8.0), and proton channels will open. In a nonvoltage-clamped cell in vivo, any I_H will tend to drive the membrane potential toward E_H, and thus the proton current is in a sense self-limiting. If no other electrogenic processes intervene, the resting potential during recovery will fall between the Nernst potentials for K^+ and H^+. Because these two conductances are of similar magnitude (10), they will compete for the privilege of controlling the resting potential. As pH_i recovers, ΔpH will dissipate, decreasing the open probability of H^+ channels and removing the driving force for H^+ current.

The effects of 10 μM Zn^{2+} strongly implicate voltage-gated proton channels in pH_i recovery from an acid load in rat type II alveolar epithelial cells in K-Ringer. Surprisingly, Zn^{2+} inhibited pH_i recovery in Ringer solution, although to a lesser extent than it did in K-Ringer. One would expect the cells to be depolarized in K-Ringer, but hyperpolarized in Ringer. Because hyperpolarization decreases the open probability of voltage-gated H^+ channels, one would expect a smaller I_H in Ringer than in K-Ringer. Two early estimates of the resting membrane potential of rat and rabbit alveolar type II epithelial cells are −27 mV (7) and −63 mV (18), respectively, based on K^+ or Rb^+ distribution. However, the assumption that the membrane potential is equivalent to the K^+ gradient neglects the fact that the voltage-gated K^+ channels identified in rat alveolar epithelial type II cells are predominantly Kv1.3 (20), which open only with depolarization above roughly −40 mV (15, 34). If Kv1.3 channels set the resting membrane potential, then it is likely to be in the vicinity of −30 to −40 mV. Then, if one assumes $\Delta pH \approx 1$, *Eq. 11* gives $I_H = 0.04–0.15$ pA/pF, much less than calculated above for $V = 0$. Yet Fig. 8 indicates that the Zn^{2+}-sensitive J_H ($qJ_H \sim I_H$) was similar in Ringer and K-Ringer at pH_o 7.4. These calculations are based on whole cell patch-clamp studies; conceivably the gating of H^+ channels in intact cells might be different. This raises the intriguing possibility that voltage-gated proton channels may be active in these cells under a wider range of conditions than previously supposed. A more mundane explanation is that the membrane potential may have become depolarized during the acid-loading procedure in Ringer solution. Because decreasing pH_i inhibits many ion channels including K^+ channels (16, 29), some depolarization in response to decreased pH_i would not be surprising. Finally, part of the explanation must be the hyperpolarization produced by proton current at low pH_i, as discussed above. These questions should be addressed in future studies using membrane potential-sensitive probes and kinetic modeling.

Zn^{2+}-insensitive pH_i recovery. To isolate the contribution of proton channels to pH_i regulation in alveolar epithelial cells, we created conditions to eliminate other transporters that might influence pH, especially those that might contribute to cytoplasmic alkalinization. The absence of Na^+ in K-Ringer prevents Na^+/H^+-antiport, at least in its normal mode of operation. Bafilomycin A_1 was used to inhibit the plasma membrane H^+-ATPase (28). We included SCH-28080 (37) to inhibit any possible H^+-K^+-ATPase activity, although this drug had no detectable effect under our conditions. This observation is consistent with the report that H^+-K^+-ATPase activity can be detected in guinea pig, but not rat, alveolar epithelium (24). We used nominally HCO_3^-- and CO_2-free conditions to avoid HCO_3^- transport. The Cl^-/HCO_3^- exchanger (33) and Cl^-/OH^- exchange (38) both normally acidify the cytoplasm and thus would not normally contribute to produce recovery from an acid load. However, if intracellular Cl^- were elevated, for example due to depolarization of the membrane potential by the high $[K^+]$ in K-Ringer, then reverse operation could conceivably produce alkalinization using environmental HCO_3^- or OH^- as a substrate. To circumvent this possibility, we also added DBDS, which inhibits anion exchangers in general and Cl^-/OH^- exchange specifically (38). Finally, to

minimize any K^+/H^+ exchange (2), we monitored pH_i recovery in Ringer plus DMA (to inhibit Na^+/H^+ antiport). Yet, even when all known transporters were inhibited or prevented from working, pH_i recovery was not prevented. Recovery was slow, with an average time constant of ~20 min in K-Ringer, but complete recovery still occurred.

The mechanism for this residual slow alkalinization is not known. Incomplete inhibition of channel-mediated H^+ efflux by Zn^{2+} is unlikely. Zn^{2+} inhibits H^+ currents by shifting $V_{threshold}$ to more positive voltages. The shift of $V_{threshold}$ by 10 μM Zn^{2+} would be 59 mV at pH_o 7.4 and 66 mV at pH 8.0 (8). Given the values of pH_{min} (Figs. 5*C* and 10*C*), $\Delta pH = 1.0$ and 1.3 at pH_o 7.4 and 8.0, respectively. From *Eq. 10*, the corresponding values of $V_{threshold}$ are −20 and −32 mV. Hence $V_{threshold}$ would be shifted by 10 μM Zn^{2+} to +39 mV at pH_o 7.4 and +34 mV at pH 8.0. Assuming that the high $[K^+]_o$ clamped the membrane potential close to 0 mV, $V_{threshold}$ for activating the proton conductance would be well positive to the membrane potential, and hence little I_H should occur. Significant H^+ permeation through the lipid bilayer is also exceedingly unlikely given the small, pH-independent leakage current measured in these cells (13). Because Cl^- was present at ~160 mM in both Ringer and K-Ringer, a recovery mechanism involving Cl^- cannot be ruled out, although any such mechanism was apparently insensitive to DBDS.

Conclusions. Voltage-gated proton channels in rat alveolar epithelial cells contribute to pH_i recovery after an acid load in normal and high-$[K^+]_o$ solutions. Slow recovery still occurred after all known transporters were inhibited, suggesting the existence of a yet-unidentified acid extrusion mechanism. Whether this mysterious transporter is the same as that deduced by Joseph et al. (22) is an open question. Zn^{2+} does not change resting pH_i, indicating that proton channels are closed under resting conditions, presumably because the membrane potential is negative to E_H. The classical property of proton channels opening only with an outward electrochemical gradient for protons ensures that there is no proton influx under normal conditions; the fundamental problem of pH regulation is acid extrusion.

ACKNOWLEDGMENTS

The authors thank Tatiana Iastrebova for excellent technical assistance.

GRANTS

This work was supported in part by Heart, Lung, and Blood Institute Grants HL-52671 and HL-61437 (to T. E. DeCoursey).

REFERENCES

1. **Adamson TM, Boyd RDH, Platt HS, and Strang LB.** Composition of alveolar liquid in the foetal lamb. *J Physiol* 204: 159–168, 1969.
2. **Attmane-Elakeb A, Boulanger H, Vernimmen C, and Bichara M.** Apical location and inhibition by arginine vasopressin of K^+/H^+ antiport of the medullary thick ascending limb of rat kidney. *J Biol Chem* 272: 25668–25677, 1997.
3. **Bevensee MO, Bashi E, and Boron WF.** Effect of trace levels of nigericin on intracellular pH and acid-base transport in rat renal mesangial cells. *J Membr Biol* 169: 131–139, 1999.
4. **Boyarsky G, Hanssen C, and Clyne LA.** Inadequacy of high K^+/nigericin for calibrating BCECF. I. Estimating steady-state intracellular pH. *Am J Physiol Cell Physiol* 271: C1131–C1145, 1996.
5. **Boyarsky G, Hanssen C, and Clyne LA.** Inadequacy of high K^+/nigericin for calibrating BCECF. II. Intracellular pH dependence of the correction. *Am J Physiol Cell Physiol* 271: C1146–C1156, 1996.
6. **Brown SES, Heming TA, Benedict CR, and Bidani A.** ATP-sensitive Na^+-H^+ antiport in type II alveolar epithelial cells. *Am J Physiol Cell Physiol* 261: C954–C963, 1991.
7. **Castranova V, Jones GS, and Miles PR.** Transmembrane potential of isolated rat alveolar type II cells. *J Appl Physiol* 54: 1511–1517, 1983.
8. **Cherny VV and DeCoursey TE.** pH-dependent inhibition of voltage-gated H^+ currents in rat alveolar epithelial cells by Zn^{2+} and other divalent cations. *J Gen Physiol* 114: 819–838, 1999.
9. **Cherny VV, Markin VS, and DeCoursey TE.** The voltage-activated hydrogen ion conductance in rat alveolar epithelial cells is determined by the pH gradient. *J Gen Physiol* 105: 861–896, 1995.
10. **DeCoursey TE.** Hydrogen ion currents in rat alveolar epithelial cells. *Biophys J* 60: 1243–1253, 1991.
11. **DeCoursey TE.** Voltage-gated proton channels and other proton transfer pathways. *Physiol Rev* 83: 475–579, 2003.
12. **DeCoursey TE and Cherny VV.** Voltage-activated proton currents in membrane patches of rat alveolar epithelial cells. *J Physiol* 489: 299–307, 1995.
13. **DeCoursey TE and Cherny VV.** Deuterium isotope effects on permeation and gating of proton channels in rat alveolar epithelium. *J Gen Physiol* 109: 415–434, 1997.
14. **DeCoursey TE and Cherny VV.** Temperature dependence of voltage-gated H^+ currents in human neutrophils, rat alveolar epithelial cells, and mammalian phagocytes. *J Gen Physiol* 112: 503–522, 1998.
15. **DeCoursey TE, Jacobs ER, and Silver MR.** Potassium currents in rat type II alveolar epithelial cells. *J Physiol* 395: 487–505, 1988.
16. **Deitmer JW and Rose CR.** pH regulation and proton signalling by glial cells. *Prog Neurobiol* 48: 73–103, 1996.
17. **Effros RM and Chinard FP.** The in vivo pH of the extravascular space of the lung. *J Clin Invest* 48: 1983–1996, 1969.
18. **Gallo RL, Finkelstein JN, and Notter RH.** Characterization of the plasma and mitochondrial membrane potentials of alveolar type II epithelial cells by the use of ionic probes. *Biochim Biophys Acta* 771: 217–227, 1984.
19. **Gerboth GD, Effros RM, Roman RJ, and Jacobs ER.** pH-induced calcium transients in type II alveolar epithelial cells. *Am J Physiol Lung Cell Mol Physiol* 264: L448–L457, 1993.
20. **Grunnet M, Rasmussen HB, Hay-Schmidt A, and Klaerke DA.** The voltage-gated potassium channel subunit, Kv1.3, is expressed in epithelia. *Biochim Biophys Acta* 1616: 85–94, 2003.
21. **Grynkiewicz G, Poenie M, and Tsien RY.** A new generation of Ca^{2+} indicators with greatly improved fluorescence properties. *J Biol Chem* 260: 3440–3450, 1985.
22. **Joseph D, Tirmizi O, Zhang XL, Crandall ED, and Lubman RL.** Polarity of alveolar epithelial cell acid-base permeability. *Am J Physiol Lung Cell Mol Physiol* 282: L675–L683, 2002.
23. **Kemp PJ, Kim KJ, Borok Z, and Crandall ED.** Re-evaluating the Na^+ conductance of adult rat alveolar type II pneumocytes: evidence for the involvement of cGMP-activated cation channels. *J Physiol* 536: 693–701, 2001.
24. **Kemp PJ, Roberts GC, and Boyd CA.** Identification and properties of pathways for K^+ transport in guinea-pig and rat alveolar epithelial type II cells. *J Physiol* 476: 79–88, 1994.
25. **Lubman RL and Crandall ED.** Na^+-HCO_3^- symport modulates intracellular pH in alveolar epithelial cells. *Am J Physiol Lung Cell Mol Physiol* 260: L555–L561, 1991.
26. **Lubman RL and Crandall ED.** Polarized distribution of Na^+-H^+ antiport activity in rat alveolar epithelial cells. *Am J Physiol Lung Cell Mol Physiol* 266: L138–L147, 1994.
27. **Lubman RL, Danto SI, Chao DC, Fricks CE, and Crandall ED.** Cl^--HCO_3^- exchanger isoform AE2 is restricted to the basolateral surface of alveolar epithelial cell monolayers. *Am J Respir Cell Mol Biol* 12: 211–219, 1995.
28. **Lubman RL, Danto SI, and Crandall ED.** Evidence for active H^+ secretion by rat alveolar epithelial cells. *Am J Physiol Lung Cell Mol Physiol* 257: L438–L445, 1989.
29. **Moody W.** Effects of intracellular H^+ on the electrical properties of excitable cells. *Annu Rev Neurosci* 7: 257–278, 1984.
30. **Negulescu PA and Machen TE.** Intracellular ion activities and membrane transport in parietal cells measured with fluorescent probes. *Methods Enzymol* 192: 38–81, 1990.
31. **Nielson DW, Goerke J, and Clements JA.** Alveolar subphase pH in the lungs of anesthetized rabbits. *Proc Natl Acad Sci USA* 78: 7119–7123, 1981.
32. **Nord EP, Brown SES, and Crandall ED.** Characterization of Na^+-H^+ antiport in type II alveolar epithelial cells. *Am J Physiol Cell Physiol* 252: C490–C498, 1987.

33. **Nord EP, Brown SES, and Crandall ED.** Cl^-/HCO_3^- exchange modulates intracellular pH in rat type II alveolar epithelial cells. *J Biol Chem* 263: 5599–5606, 1988.
34. **Peers C, Kemp PJ, Boyd CAR, and Nye PCG.** Whole-cell K^+ currents in type II pneumocytes freshly isolated from rat lung: pharmacological evidence for two subpopulations of cells. *Biochim Biophys Acta* 1052: 113–118, 1990.
35. **Roos A and Boron WF.** Intracellular pH. *Physiol Rev* 61: 296–434, 1981.
36. **Sano K, Cott GR, Voelker DR, and Mason RJ.** The Na^+/H^+ antiporter in rat alveolar type II cells and its role in stimulated surfactant secretion. *Biochim Biophys Acta* 939: 449–458, 1988.
37. **Scott CK and Sundell E.** Inhibition of H^+K^+ATPase by SCH 28080 and SCH 32651. *Eur J Pharmacol* 112: 268–270, 1985.
38. **Sun B, Leem CH, and Vaughan-Jones RD.** Novel chloride-dependent acid loader in the guinea-pig ventricular myocyte: part of a dual acid-loading mechanism. *J Physiol* 15: 65–82, 1996.
39. **Thomas JA, Buchsaum RN, Zimniak A, and Racker E.** Intracellular pH measurements in Ehrlich ascites tumor cells utilizing spectroscopic probes generated in situ. *Biochemistry* 18: 2210–2218, 1979.
40. **Walpole RE and Myers RH.** *Probability and Statistics for Engineers and Scientists.* New York: Macmillan, 1978, p. 580.